Chapter 7
Practical Reliability Analysis of Slope Stability by Advanced Monte Carlo Simulations in a Spreadsheet

7.1 Introduction

The previous chapters developed several probabilistic approaches for geotechnical site characterization. These probabilistic approaches provide probabilistic characterization of soil properties and underground stratigraphy and account rationally for inherent spatial variability of soils and various uncertainties (i.e., statistical uncertainties, measurement errors, and transformation uncertainties) that arise during site characterization. The uncertainties (including inherent spatial variability of soils) obviously affect probabilistic estimations of soil properties and underground stratigraphy, which are key input information in probabilistic analysis and/or designs of geotechnical structures. Therefore, the uncertainties subsequently influence probabilistic analysis and/or designs of geotechnical structures. Consider, for example, probabilistic slope stability analysis. Various uncertainties can be taken into account rationally in probabilistic slope stability analysis through Monte Carlo simulation (MCS). MCS method provides a robust and conceptually simple way to estimate the "reliability index" β or slope failure probability P_f (e.g., El-Ramly et al. 2002; Griffiths and Fenton 2004; El-Ramly et al. 2005). Direct MCS, however, suffers from a lack of efficiency and resolution at small probability levels that are of great interest to geotechnical practitioners (see Chap. 2).

In addition, it has been recognized that a slope may fail along an unlimited number of potential slip surfaces, although evaluating the total failure probability along all potential slip surfaces is considered a mathematically formidable task (El-Ramly et al. 2002). The value of β for slope stability therefore is frequently determined only for one or a limited number of slip surfaces (e.g., Tang et al. 1976; Hassan and Wolff 1999; El-Ramly et al. 2002). A few exceptions are the recent work by Griffiths and Fenton (2004), Xu and Low (2006), and Hong and Roh (2008) that utilize direct MCS and finite element analysis to search for the critical slip surfaces. Nevertheless, the effect of critical slip surface uncertainty has not been explored systematically.

Z. Cao et al., *Probabilistic Approaches for Geotechnical Site Characterization and Slope Stability Analysis*, DOI 10.1007/978-3-662-52914-0_7

This chapter presents a practical approach of slope stability–reliability analysis that implements an advanced MCS method called "subset simulation" in a spreadsheet environment for improving the efficiency and resolution of MCS at relatively small probability levels and for exploring the effect of critical slip surface uncertainty. MCS and subset simulation are operationally decoupled from deterministic slope stability analysis and implemented using a commonly available spreadsheet software, Microsoft Excel. The proposed methodology is illustrated through application to a cohesive slope and validated against results from other reliability solution methods and commercial software. With the aid of improved computational efficiency and resolution at relatively small probability levels offered by the proposed methodology, the effects of inherent spatial variability of soil property and critical slip surface uncertainty will be explored.

7.2 Monte Carlo Simulation of Slope Stability

Figure 7.1 shows a flowchart for MCS of slope stability analysis schematically. The MCS starts with characterization of probability distributions of uncertainties concerned, as well as slope geometry and other necessary information, followed by the generation of n_{MC} sets of random samples according to the prescribed probability distributions. Note that the input information required (e.g., probability distributions of soil properties) in MCS can be obtained from probabilistic approaches developed for geotechnical site characterization in the previous four chapters. For each set of random samples, limit equilibrium methods are utilized, and the critical slip surface is searched for obtaining the minimum FS, resulting in totally n_{MC} sets of minimum FS. Then, statistical analysis is performed to estimate P_f or β, with the slope failure defined as the minimum $FS < 1$. To ensure a desired level of accuracy in P_f, the number of samples in direct MCS should be at least ten times greater than the reciprocal of the probability level of interest (Robert and Casella 2004). For a P_f level of 0.001 that corresponds to an expected performance level of "above average" (see Table 2.7 in Chap. 2), the sample sizes of direct MCS should be greater than 10,000. As the deterministic slope stability analysis explicitly searches a wide range of potential slip surfaces to obtain the minimum FS, direct MCS takes considerable amount of time. This further calls for improvement of computational efficiency via advanced Monte Carlo procedures as presented in the following section.

7.3 Subset Simulation

Subset simulation (Au and Beck 2001, 2003) stems from the idea that a small failure probability can be expressed as a product of larger conditional failure probabilities for some intermediate failure events, thereby converting a rare event

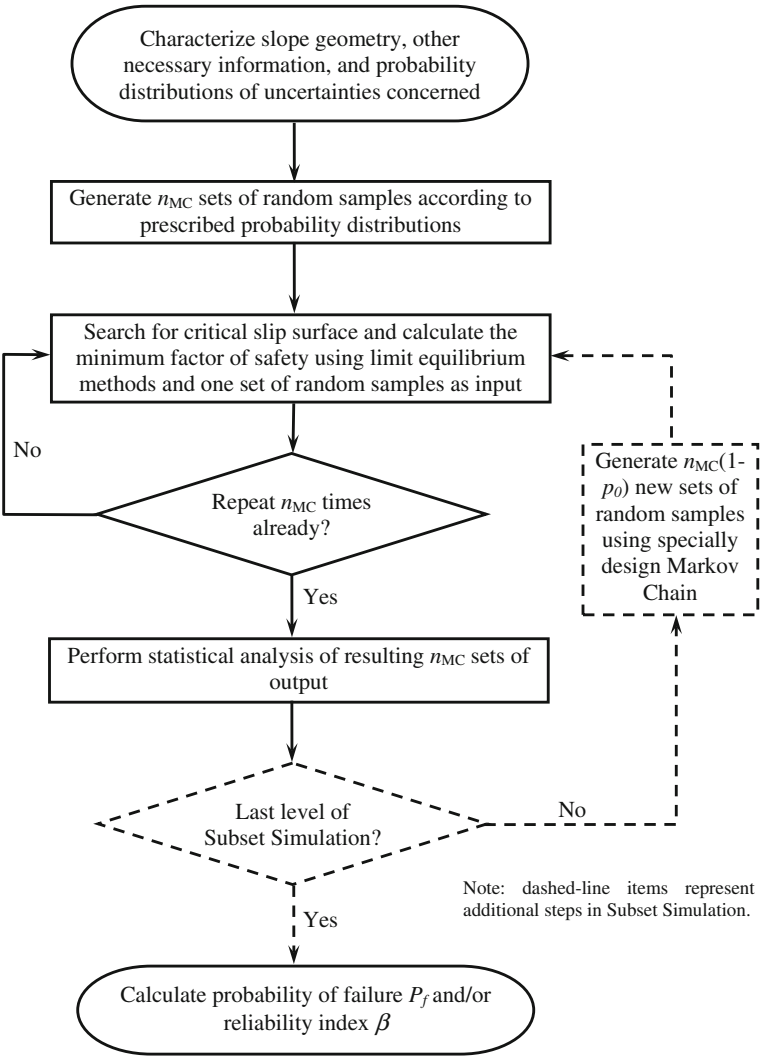

Fig. 7.1 Flowchart for Monte Carlo simulation of slope stability analysis (after Wang et al. 2011)

(small probability levels) simulation problem into a sequence of more frequent ones. Consider the slope stability problem where FS is the critical response and the probability of FS smaller than a given value "fs" (i.e., $P(FS < fs)$) is of interest. Let $fs = fs_m < fs_{m-1} < \cdots fs_2 < fs_1$ be an increasing sequence of m intermediate threshold values. By sequentially conditioning on the event $\{F_i = FS < fs_i, i = 1, 2, \ldots, m\}$, the probability $P(FS < fs)$ can be written as

$$P(FS < fs) = P(FS < fs_1)P(FS < fs_2 | FS < fs_1) \times \cdots \times P(FS < fs_m | FS < fs_{m-1}) \tag{7.1}$$

In implementation, $fs_1, \ldots, fs_m$ are determined adaptively based on the statistical analysis of simulation output (as shown by the dashed-line items in Fig. 7.1) so that the sample estimates of $P(FS < fs_1)$ and $\{P(FS < fs_i | FS < fs_{i-1}),\ i = 2, \ldots, m\}$ always correspond to a common specified value of the conditional probability p_0 ($p_0 = 0.1$ is found to be a good choice) (Au et al. 2009 and 2010).

The efficient generation of conditional samples is pivotal in the success of subset simulation, and it is made possible through the machinery of Markov Chain Monte Carlo simulation (MCMCS). MCMCS uses a modified version of the Metropolis algorithm (Metropolis et al. 1953) that is applicable for high-dimensional problems. Successive samples are generated from a specially designed Markov Chain whose limiting stationary distribution tends to the target probability distribution function (PDF) as the length of the Markov Chain increases. Details of the modified Metropolis algorithm of MCMCS are referred to Au and Beck (2001 and 2003) and Au et al. (2007).

7.4 Implementation of Subset Simulation in a Spreadsheet Environment

The subset simulation described above has been implemented in a commonly available spreadsheet environment by a package of worksheets and functions/Add-In in Excel with the aid of Visual Basic for Application (VBA) (Au et al. 2009; Au et al. 2010; Wang et al. 2011). It is of particular interest to decouple the development of Excel worksheets and VBA functions/Add-In for deterministic slope stability analysis and those for reliability analysis (e.g., random sample generations and statistical analysis) so that the reliability analysis can proceed as an extension of deterministic analysis in a non-intrusive manner. This allows the deterministic analysis of slope stability and reliability analysis to be performed separately by personnel with different expertise and in a parallel fashion. This alleviates the geotechnical practitioners from performing reliability computational algorithms so that they can focus on the slope stability problem itself. The software package developed in this chapter therefore is divided into three parts: deterministic model worksheet for deterministic analysis of slope stability, uncertainty model worksheet for generating random samples, and subset simulation Add-In for uncertainty propagation, which are described in the following three subsections, respectively.

7.4.1 Deterministic Model Worksheet

For a slope stability problem, deterministic model analysis is the process of calculating factor of safety (i.e., *FS*) for a given nominal set of values of system parameters. The system parameters include the geometry information of the slope and the slip surface, soil properties, and profile of soil layers. In this chapter, limit equilibrium methods (e.g., Swedish circle method, simplified Bishop method, and Spencer method) (Duncan and Wright 2005) are employed to calculate the factor of safety for the critical slip surface. The calculation process of deterministic analysis is implemented in a series of worksheets assisted by some VBA functions/Add-In. Figure 7.2 illustrates an example of deterministic model worksheet which is modified after Low (2003) and uses Ordinary Method of Slices. The worksheet is

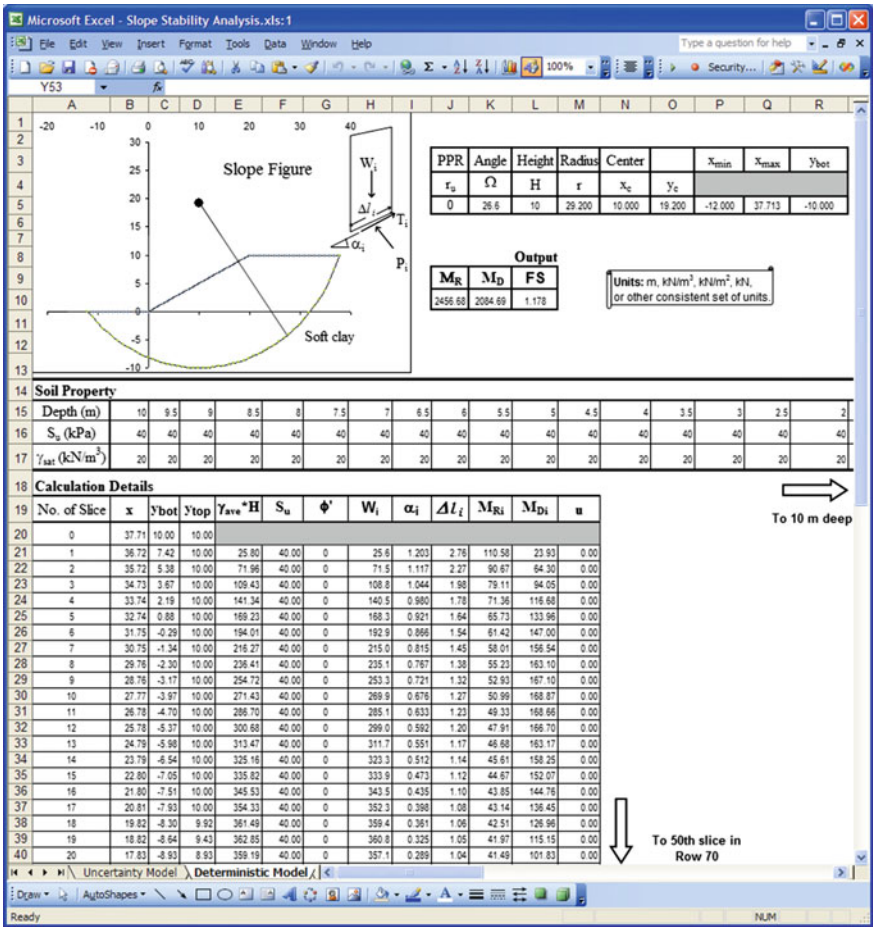

Fig. 7.2 Deterministic model worksheet for slope stability analysis (after Au et al. 2010)

divided into three parts: slope geometry and *FS* calculation (i.e., Rows 1–13), soil property profiles (Rows 14–17), and calculation details for each slice (Rows 18–70). For a given slip surface defined by radius (i.e., Cell M5) and center coordinates (i.e., Cell N5 and Cell O5), a *FS* (i.e., Cell L10) can be calculated accordingly. A wide range of combinations of slip surface radius and center coordinates are then searched explicitly to obtain the minimum *FS* and its corresponding critical slip surface. From an input–output perspective, the deterministic analysis worksheets take a given set of values (e.g., Row 16 in Fig. 7.2) as input, calculate the factor of safety, and return the factor of safety as an output.

7.4.2 Uncertainty Model Worksheet

An uncertainty model worksheet is developed to generate random samples of uncertain system parameters that are treated as random variables in the analysis. The uncertain worksheet includes detailed information of random variables, such as statistics, distribution type, and correlation information. The generation of random samples starts with an Excel built-in function "RAND()" for generating uniform random samples, which are then transformed to random samples of the target distribution type (e.g., normal distribution or lognormal distribution). If the random variables are considered correlated, Cholesky factorization of the correlation matrix is performed to obtain a lower triangular matrix, which is used in the transformation to generate correlated random samples. Figure 7.3 shows an example of uncertainty model worksheet, which consists of three parts: a variable description zone (i.e., Rows 2–5), a random sample generation zone (i.e., Rows 6–13), and a zone showing a lower triangular matrix obtained from Cholesky factorization of the correlation matrix (i.e., Rows 14–54). From the input–output perspective, the uncertainty model worksheet takes no input but returns a set of random samples (e.g., Row 13 in Fig. 7.3) of the uncertain system parameters as its output.

When deterministic model worksheet and uncertainty model worksheet are developed, they are linked together through their input/output cells (e.g., Row 16 in Fig. 7.2 and Row 13 in Fig. 7.3) to execute probabilistic analysis of slope stability. The connection is carried out by simply setting the cell references for nominal values of uncertain parameters in deterministic model worksheet to be the cell references for the random samples in the uncertainty model worksheet in Excel. After this task, the values of uncertain system parameters shown in the deterministic model worksheet are equal to that generated in the uncertainty model worksheet, and so the values of the safety factor calculated in the deterministic model worksheet are random.

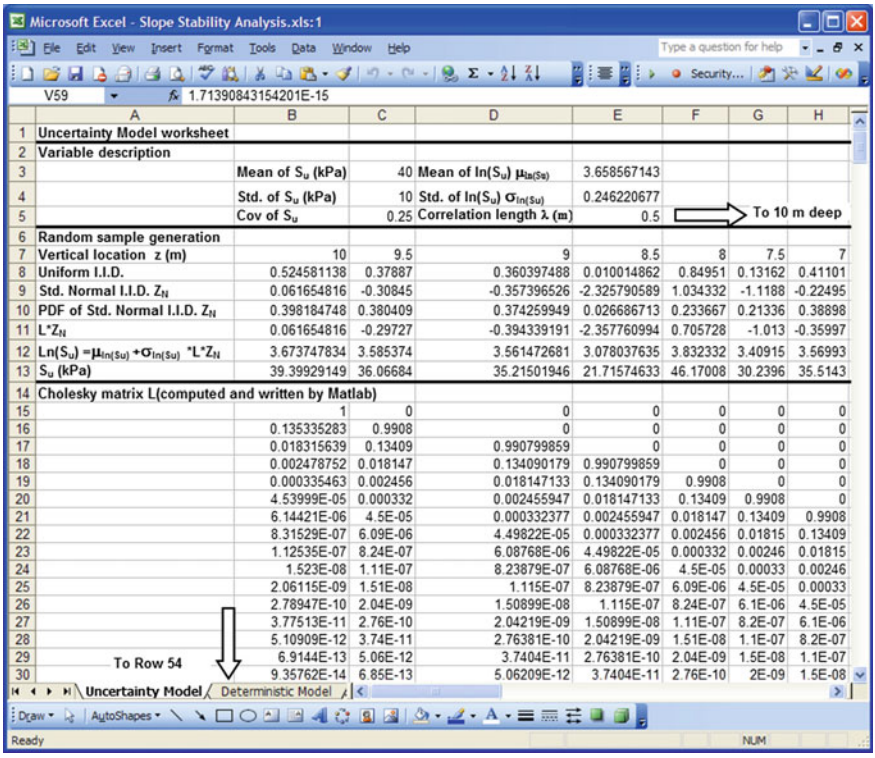

	A	B	C	D	E	F	G	H
1	Uncertainty Model worksheet							
2	Variable description							
3		Mean of S_u (kPa)	40	Mean of ln(S_u) $\mu_{ln(Su)}$	3.658567143			
4		Std. of S_u (kPa)	10	Std. of ln(S_u) $\sigma_{ln(Su)}$	0.246220677			
5		Cov of S_u	0.25	Correlation length λ (m)	0.5			
6	Random sample generation							
7	Vertical location z (m)	10	9.5	9	8.5	8	7.5	7
8	Uniform I.I.D.	0.524581138	0.37887	0.360397488	0.010014862	0.84951	0.13162	0.41101
9	Std. Normal I.I.D. Z_N	0.061654816	-0.30845	-0.357396526	-2.325790589	1.034332	-1.1188	-0.22495
10	PDF of Std. Normal I.I.D. Z_N	0.398184748	0.380409	0.374259949	0.026686713	0.233667	0.21336	0.38898
11	L*Z_N	0.061654816	-0.29727	-0.394339191	-2.357760994	0.705728	-1.013	-0.35997
12	Ln(S_u) =$\mu_{ln(Su)}$ +$\sigma_{ln(Su)}$ *L*Z_N	3.673747834	3.585374	3.561472681	3.078037635	3.832332	3.40915	3.56993
13	S_u (kPa)	39.39929149	36.06684	35.21501946	21.71574633	46.17008	30.2396	35.5143
14	Cholesky matrix L(computed and written by Matlab)							
15		1	0	0	0	0	0	0
16		0.135335283	0.9908	0	0	0	0	0
17		0.018315639	0.13409	0.990799859	0	0	0	0
18		0.002478752	0.018147	0.134090179	0.990799859	0	0	0
19		0.000335463	0.002456	0.018147133	0.134090179	0.9908	0	0
20		4.53999E-05	0.000332	0.002455947	0.018147133	0.13409	0.9908	0
21		6.14421E-06	4.5E-05	0.000332377	0.002455947	0.018147	0.13409	0.9908
22		8.31529E-07	6.09E-06	4.49822E-05	0.000332377	0.002456	0.01815	0.13409
23		1.12535E-07	8.24E-07	6.08768E-06	4.49822E-05	0.000332	0.00246	0.01815
24		1.523E-08	1.11E-07	8.23879E-07	6.08768E-06	4.5E-05	0.00033	0.00246
25		2.06115E-09	1.51E-08	1.115E-07	8.23879E-07	6.09E-06	4.5E-05	0.00033
26		2.78947E-10	2.04E-09	1.50899E-08	1.115E-07	8.24E-07	6.1E-06	4.5E-05
27		3.77513E-11	2.76E-10	2.04219E-09	1.50899E-08	1.11E-07	8.2E-07	6.1E-06
28		5.10909E-12	3.74E-11	2.76381E-10	2.04219E-09	1.51E-08	1.1E-07	8.2E-07
29		6.9144E-13	5.06E-12	3.7404E-11	2.76381E-10	2.04E-09	1.5E-08	1.1E-07
30		9.35762E-14	6.85E-13	5.06209E-12	3.7404E-11	2.76E-10	2E-09	1.5E-08

Fig. 7.3 Uncertainty model worksheet (after Au et al. 2010)

7.4.3 Subset Simulation Add-In

When the deterministic analysis and uncertainty model worksheets are completed and linked together, subset simulation procedure is invoked for uncertainty propagation. In this chapter, subset simulation is implemented as an Add-In in Excel (Au et al. 2009, 2010). The userform of the Add-In is shown in Fig. 7.4. The upper four input fields of the userform (i.e., number of subset simulation runs, number of samples per level N, conditional probability from one level to next p_0, and the highest subset simulation level m) control the number of samples generated by subset simulation. The total number of samples per subset simulation run is equal to $N + mN\ (1 - p_0)$. The lower four input fields of the userform record the cell references of the random variables, their PDF values, and the cell references of the system response (e.g., $Y = 1/FS$) and other variables V (e.g., random samples) of interest, respectively.

After each simulation run, the Add-In provides the complementary cumulative density function (CDF) of the driving variable versus the threshold level, i.e.,

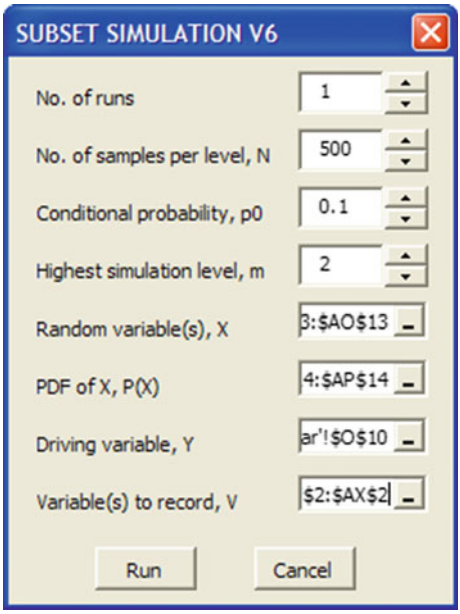

Fig. 7.4 The userform of subset simulation Add-In (after Au et al. 2010; Wang and Cao 2013)

estimate for *P(Y > 1/fs)* versus *1/fs*, into a new spreadsheet and produces a plot of it. Then, the CDF, histograms, or conditional counterparts of uncertain parameters of interest can be calculated using the output information obtained.

7.5 Illustrative Example

The proposed methodology and Excel spreadsheet package developed are applied to assess the reliability of short-term stability of a cohesive soil slope as shown in Fig. 7.5. The cohesive soil slope has a height H = 10 m and slope angle of 26.6º, corresponding to an inclination ratio of 1:2. The cohesive soil is underlain by a firm stratum at 20 m below top of the slope. Short-term shear strength of the cohesive soil is characterized by undrained shear strength S_u, and the saturated unit weight of soil is γ_{sat}. Short-term stability of the slope is assessed using Ordinary Method of Slices under undrained condition (Duncan and Wright 2005). The factor of safety FS is defined as the minimum ratio of resisting moment over the overturning moment, and the slip surface is assumed to be a circular arc centered at coordinate (x_c, y_c) and with radius r. As shown in Fig. 7.5, the soil mass above the slip surface is divided into a number of vertical slices, each of which has a weight W_i, circular slip segment length Δl_i, undrained shear strength S_{ui} along the slip segment, and an angle α_i between the base of the slice and the horizontal. The FS is then given by

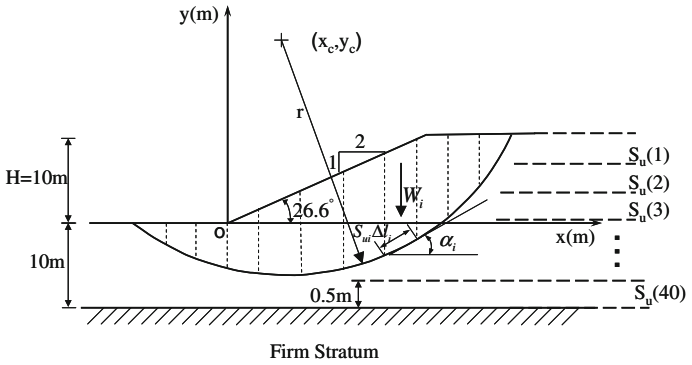

Fig. 7.5 A cohesive soil slope example (after Wang et al. 2011)

$$FS = \min_{x_c, y_c, r} \frac{\sum S_{ui} \Delta l_i}{\sum W_i \sin \alpha_i} \tag{7.2}$$

where the minimum is taken over all possible slip circles, i.e., all possible choices of (x_c, y_c) and r. Note that Δl_i, W_i, and α_i change as (x_c, y_c) and/or r change (i.e., geometry of the ith slice changes). In addition, the W_i is a function of the soil saturated unit weight γ_{sat}. FS therefore depends on geometry of slip surface (i.e., (x_c, y_c) and r) and soil properties (i.e., S_u and γ_{sat}), and S_{ui} and γ_{sat} are key input variables as described in the following subsection.

7.5.1 Input Variables

The undrained shear strength S_u of soil is modeled by a one-dimensional random field spatially varying along the vertical direction. The value of S_u at the same depth is assumed to be fully correlated. The inherent spatial variability with depth is modeled by a homogeneous lognormal random field with an exponentially decaying correlation structure. Let $S_u(D_i)$ be the value of undrained shear strength at depth D_i. The correlation R_{ij} between $\ln[S_u(D_i)]$ and $\ln[S_u(D_j)]$ at respective depths D_i and D_j is given by

$$R_{ij} = \exp(-2|\mathrm{D_i} - \mathrm{D_j}|/\lambda) \tag{7.3}$$

where λ is the effective correlation length. As implied by this correlation function, when $|D_i - D_j| \geq \lambda$, $\ln[S_u(D_i)]$ and $\ln[S_u(D_j)]$ are effectively uncorrelated (Vanmarcke 1977, 1983). When $|D_i - \mathrm{D_j}|$ is much smaller than λ, $\ln[S_u(D_i)]$ and $\ln[S_u(D_j)]$ are highly correlated. In this example, the value of λ varies from 0.5 m to infinity for consideration of different spatial correlations. As shown in Fig. 7.5, the

Table 7.1 The values and distributions of the input variables (after Wang et al. 2011)

Variable	Distribution	Statistics
$\underline{S_u}$	Lognormal (a vector with a length of 40)	Mean = 40 kPa COV[a] = 25 % λ varies from 0.5 m to $+\infty$
γ_{sat}	Deterministic	20 kN/m^3

[a] "COV" stands for coefficient of variation

20-m-thick cohesive soil layer is divided into forty 0.5-m-thick sublayers, and S_u at each sublayer is represented by an entry in a $\underline{S_u}$ vector with a length of 40. Table 7.1 summarizes the material parameters and their variability used in the analysis. The mean and standard deviation of S_u are approximately equal to 40 and 10 kPa (i.e., 25 % coefficient of variation (COV)), respectively. The saturated unit weight of cohesive soil γ_{sat} is taken as deterministic with a value of 20 kN/m^3. As a reference, the nominal value of FS that corresponds to the case where all S_u values equal to their mean values of 40 kPa is equal to 1.178.

7.5.2 Simulation Results

Table 7.2 summarizes the results of both direct MCS and subset simulation for $\lambda = +\infty$ and 0.5 m, respectively. When $\lambda = +\infty$, all 40 entries in the $\underline{S_u}$ vector are fully correlated, and they are equivalent to a single random variable. Both direct MCS and subset simulation provide a consistent P_f value of about 30 %, which compares well with the P_f value given by Griffiths and Fenton (2004) for cohesive slopes with similar geometry and soil properties. When $\lambda = 0.5$ m, all 40 entries in the $\underline{S_u}$ vector can be approximated as 40 independent and identically distributed random variables. Direct MCS and subset simulation provide a consistent P_f value of about 0.9 %, which is significantly smaller than the one for $\lambda = +\infty$. This is

Table 7.2 Summary of simulation results (after Wang et al. 2011)

Effective correlation length λ (m)	Simulation method	Number of samples	Reliability index β[a]	Probability of failure P_f (%)
$+\infty$	Direct MCS	1000	0.52	30
$+\infty$	Subset simulation	200 + 180 + 180 = 560	0.55	29
0.5	Direct MCS	2000	2.35	0.95
0.5	Subset simulation	500 + 450 + 450 = 1400	2.36	0.92

[a]Equivalent reliability index $\beta = \Phi^{-1}(1 - P_f)$ where Φ = standard normal cumulative distribution function

consistent with the observation by Hong and Roh (2008) that P_f decreases if spatial correlation is ignored (i.e., as λ decreases). The effect of inherent spatial variability is discussed further in a later section of this chapter.

As the value of P_f decreases to a relatively small level (e.g., around 0.9 % for λ = 0.5 m), the number of samples required in direct MCS increases significantly and efficiency of direct MCS decreases dramatically. Figure 7.6 shows a histogram of the *FS* from 2000 direct MCS samples, among which 19 samples have a $FS < 1$. The efficiency of simulating failure events (i.e., $FS < 1$) is relatively low. The resolution of P_f is 1/2000 = 0.05 %, and this resolution might not be sufficient for a P_f value of 0.95 %.

In contrast, Fig. 7.7 shows histograms of the *FS* from three levels of subset simulation with a p_0 value of 0.1. The first level of subset simulation is equivalent to a direct MCS with a sample number of 500, and only 2 samples have a $FS < 1$, as shown in Fig. 7.7a. All 500 *FS* values are then sorted in a decreasing order, and 50 samples (i.e., 10 % (or $p_0 = 0.1$) of 500 samples) with the lowest *FS* are used to generate 450 samples in the second level of subset simulation, as illustrated by the dashed-line items in Fig. 7.1. As shown in Fig. 7.7b, the samples at the second level fall into the region of $FS < 1.06$ and have relatively small *FS* values. Forty-four samples out of 450 samples have a $FS < 1$, and the efficiency of simulating failure events improves significantly when compared with direct MCS. As shown in Fig. 7.7c, the samples at the third level move further to the lower *FS* region, and 413 samples out of 450 samples have a $FS < 1$. The P_f is calculated as $0.1 \times 0.1 \times 413/450 = 0.92$ %, and the resolution of P_f is $0.1 \times 0.1 \times 1/450 = 0.002$ %. Subset simulation significantly improves efficiency and resolution of simulations at small probability levels. Such improvement becomes increasingly substantial and necessary as the probability level of interest decreases (e.g., P_f further decreases to 0.1 % or 0.003 % for expected performance levels of "above

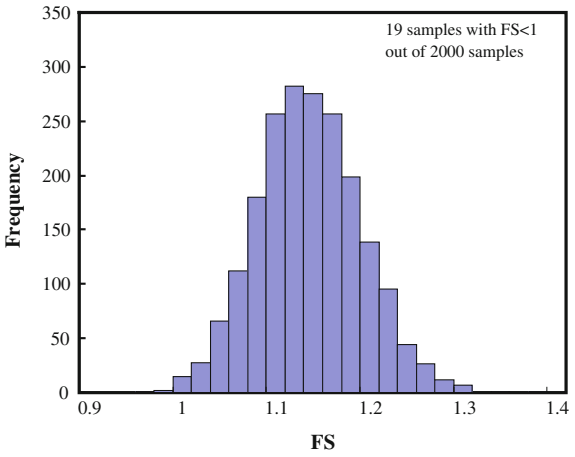

Fig. 7.6 *FS* histogram from direct Monte Carlo simulation (after Wang et al. 2011)

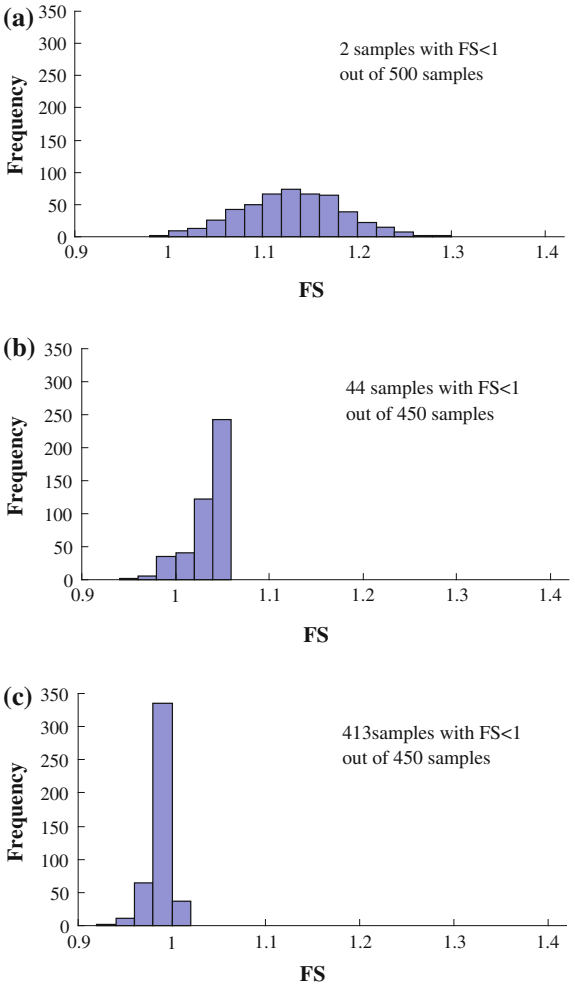

Fig. 7.7 *FS* histogram from subset simulation (after Wang et al. 2011). **a** First level. **b** Second level. **c** Third level

average" or "good" (see Table 2.7 in Chap. 2), respectively, as direct MCS is increasingly inefficient).

7.5.3 Comparison with Other Reliability Analysis Methods

The analysis results are compared with those from other reliability analysis methods, including the first-order second-moment method (FOSM), first-order reliability method (FORM), and direct MCS using commercial software Slope/W (GEO-SLOPE International Ltd. 2008). Table 7.3 summarizes analysis results from different reliability methods with $\lambda = +\infty$. The value of P_f varies from about 27 to 30 % with a maximum relative difference of 10 % among difference methods.

Table 7.3 Summary of analysis results from different reliability methods ($\lambda = +\infty$) (after Wang et al. 2011)

Reliability method	Reliability index β	Probability of failure P_f (%)	Relative difference in P_f (%)
FOSM	0.61	27	−10
FORM	0.55	29	−3
Direct MCS with Slope/W	0.55	29	−3
Direct MCS with Excel	0.52	30	N/A
Subset simulation with Excel	0.55	29	−3

Table 7.4 Summary of analysis results from different reliability methods ($\lambda = 0.5$ m) (after Wang et al. 2011)

Reliability method	Reliability index β	Probability of failure P_f (%)	Relative difference in P_f (%)
FOSM	2.53	0.57	−40
FORM	2.61	0.45	−53
Direct MCS with Slope/W	2.80	0.26	−73
Direct MCS with Excel	2.35	0.95	N/A
Subset simulation with Excel	2.36	0.92	−3

The results from direct MCS or subset simulations compare favorably with those from FOSM, FORM, or direct MCS using Slope/W. Table 7.4 summarizes similar results for $\lambda = 0.5$ m. The value of P_f varies from 0.26 to 0.95 %, which is significantly smaller than those for $\lambda = +\infty$. The maximum relative difference among different methods for $\lambda = 0.5$ m is about 73 %, which is significantly larger than that for $\lambda = +\infty$. These differences can be attributed to calculation details of each reliability analysis method, inherent spatial variability of soil property, and critical slip surface uncertainty, which are discussed in the following several sections.

7.6 Calculation Details of Other Reliability Analysis Methods

7.6.1 First-Order Second-Moment Method (FOSM)

FOSM uses the first-order terms of a Taylor series expansion of *FS* with respect to the random variables, and it is frequently performed with a fixed critical slip surface (e.g., Ang and Tang 1984; Tang et al. 1976; Wu 2008). Consistent with the previous studies, the critical slip surface here is determined by setting all $\underline{S_u}$ values

equal to their mean values of 40 kPa and searching for the minimum FS. The resulting critical slip surface has an r = 29.2 m and (x_c, y_c) = (10.0 m, 19.2 m), and the corresponding FS is 1.178. The mean and standard deviation of FS are then estimated for both cases of λ =+∞ and λ = 0.5 m. Note that, when λ =+∞, all 40 entries in the $\underline{S_u}$ vector are fully correlated, and all S_{ui} behave as a single random variable S_u. Equation (7.2) then can be rewritten as

$$FS = \min_{x_c,y_c,r} \frac{\sum S_{ui}\Delta l_i}{\sum W_i \sin\alpha_i} = \min_{x_c,y_c,r} \frac{S_u \sum \Delta l_i}{\sum W_i \sin\alpha_i} = S_u \min_{x_c,y_c,r} \frac{\sum \Delta l_i}{\sum W_i \sin\alpha_i} \tag{7.4}$$

As the geometry and soil unit weight are considered deterministic, $\min_{x_c,y_c,r} \frac{\sum \Delta l_i}{\sum W_i \sin\alpha_i}$ is deterministic. Equation (7.4) implies that when λ = +∞ (i.e., inherent spatial variability is ignored or perfect correlation), location of critical slip surface (i.e., x_c, y_c, and r) is independent of the value of S_u, although the value of minimum FS does vary as the S_u value changes. In this case, it is theoretically appropriate that FOSM method only uses a given slip surface in the analysis. In contrast, when λ = 0.5 m (i.e., inherent spatial variability is considered), all 40 S_{ui} are random variables. Critical slip surface (i.e., x_c, y_c, and r) varies spatially and is uncertain, depending on the value of S_{ui}. Using only one given critical slip surface in FOSM method therefore underestimates the uncertainty of failure. This results in significant increase of relative difference in P_f between FOSM method and direct MCS with Excel from Table 7.3 (i.e., −10 % for λ = +∞) to Table 7.4 (i.e., −40 % for λ = 0.5 m). The effect of critical slip surface uncertainty is discussed further under the Sect. 7.8 "Effect of Critical Slip Surface Uncertainty".

7.6.2 *First-Order Reliability Method (FORM)*

The reliability index β for FORM in Tables 7.3 and 7.4 is calculated using an Excel spreadsheet with its built-in optimization tool "Solver" to obtain the minimum distance of interest as β (Low and Tang 2007; Low 2003). Although this FORM approach is mathematically sound, its successful application relies on a robust optimization algorithm for multidimensional minimization. Similar to other optimization algorithm, the generalized reduced gradient algorithm used in the Excel "Solver" might not result in a global minimum but a local minimum, particularly when the function of interest is complex and dimension of the space is high. One frequently used heuristic for checking if the global minimum is obtained is simply repeating the optimization with widely varying starting points. The β values for FORM in Tables 7.3 and 7.4 are obtained with a starting point that corresponds to the critical slip surface obtained from a deterministic slope stability analysis with all soil properties equal to their respective mean values (Low 2003). When the optimization is repeated with a slightly different starting point (e.g., different slip surface parameters or soil properties), the Excel "Solver" gives significantly

different β value, or even fails to converge. The value of β given by the Excel "Solver" should, therefore, be treated with caution, and it may correspond to a local minimum that is larger than the global minimum (i.e., the true β value). In other words, the FORM overestimates the β value or underestimates the P_f value, which is unconservative and undesirable. This observation is consistent with the results summarized in Tables 7.3 and 7.4. The β values for both cases of $\lambda = +\infty$ and $\lambda = 0.5$ m are larger than those from direct MCS with Excel. Note that FORM's overestimation of β is not unique for slope stability problem. Similar observations are also reported by Ching et al. (2009) for consolidation problem.

7.6.3 *Monte Carlo Simulations Using Commercial Software Slope/W*

The commercial software Slope/W (GEO-SLOPE International Ltd. 2008) is first used to perform a deterministic slope stability analysis with all $\underline{S_u}$ values equal to their mean values of 40 kPa. The resulting minimum *FS* (i.e., 1.178) and critical slip surface (i.e., $r = 29.0$ m and $(x_c, y_c) = (9.9$ m, 19.0 m)) are virtually identical to those obtained from the Excel spreadsheet. Monte Carlo simulations are then performed using Slope/W for both cases of $\lambda = +\infty$ and $\lambda = 0.5$ m. When $\lambda = +\infty$, the relative difference in P_f between direct MCS from Slope/W and Excel is within 3 % (see Table 7.3). When λ decreases to 0.5 m, the relative difference in P_f increases to 73 % (see Table 7.4). The relatively large difference can be attributed to the way that Slope/W handles the critical slip surface in direct MCS. Slope/W uses only one given critical slip surface in direct MCS, and the given slip surface is determined based on a deterministic slope stability analysis with all random variables equal to their respective mean values. Figure 7.8 shows the critical slip surface obtained in Slope/W using the mean values of $\underline{S_u}$. As discussed under the Sect. 7.6.1 "first-order second-moment method (FOSM)," when $\lambda = +\infty$ (i.e., inherent spatial variability is ignored), it is theoretically appropriate to use only one given critical slip surface. The direct MCS in Slope/W therefore gives reasonable result, and the relative difference in P_f between direct MCS from Slope/W and Excel is small. When $\lambda = 0.5$ m (i.e., inherent spatial variability is considered), the critical slip surface itself varies spatially. Using only one given critical slip surface in direct MCS with Slope/W therefore underestimates the P_f, and the relative difference in P_f between direct MCS from Slope/W and Excel increases significantly (see Table 7.4). The effects of inherent spatial variability of soil property and critical slip surface uncertainty are discussed in two following sections, respectively.

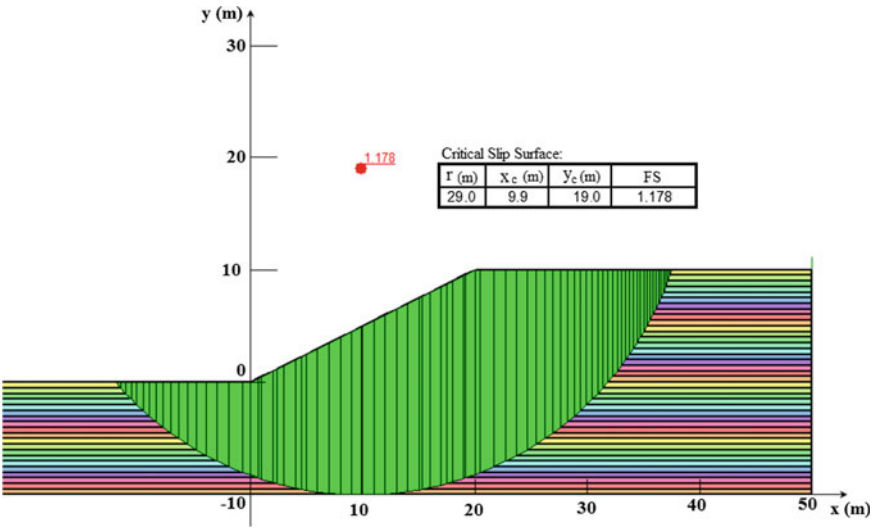

Fig. 7.8 Critical slip surface in Slope/W (after Wang et al. 2011)

7.7 Effect of Inherent Spatial Variability of Soil Property

A series of direct MCS and subset simulations with different λ values are performed using the Excel spreadsheet package developed in this chapter. Figure 7.9 summarizes the results in a plot of P_f versus normalized correlation length (λ/H). As λ/H increases from 0.05 to 1 (or λ increases from 0.5 to 10 m for H = 10 m), the value of P_f increases significantly from about 0.9 to 26 %. When $\lambda/H > 1$ or λ is larger than the slope height H, the effect of λ on P_f begins to diminish, and P_f varies slightly as λ/H further increases. If the soil properties (e.g., S_u) are characterized by a single random variable or the inherent spatial variability is ignored, the value of P_f is overestimated significantly, particularly when the effective correlation length is smaller than the slope height.

Note that FS is defined as the minimum ratio of summation of resisting moments over the summation of overturning moments (see Eq. (7.2)) and slope failure occurs when $FS < 1$. Let M_R be a summation of n_R resisting moments $\Delta l_i S_{ui}$ (i.e., $M_R = \sum_{i=1}^{n_R} \Delta l_i S_{ui}$) and variance of M_R then can be expressed as

$$Var(M_R) = \sum_{i=1}^{n_R} \Delta l_i^2 \sigma_{S_{ui}}^2 + \sum_{i,j=1}^{n_R} \sum_{i \neq j}^{n_R} \rho_{ij} \Delta l_i \Delta l_j \sigma_{S_{ui}} \sigma_{S_{uj}} \tag{7.5}$$

where $\sigma_{S_{ui}}^2$ is variance of S_{ui} and ρ_{ij} is correlation coefficient between S_{ui} and S_{uj}. The effect of inherent spatial variability is reflected by the variation of ρ_{ij} (i.e., between 0 and 1) and the second term at the right-hand side of Eq. (7.5), i.e., $\sum_{i,j=1}^{n_R} \sum_{i \neq j}^{n_R} \rho_{ij} \Delta l_i \Delta l_j \sigma_{S_{ui}} \sigma_{S_{uj}}$. When S_{ui} and S_{uj} are uncorrelated, $\rho_{ij} = 0$ and

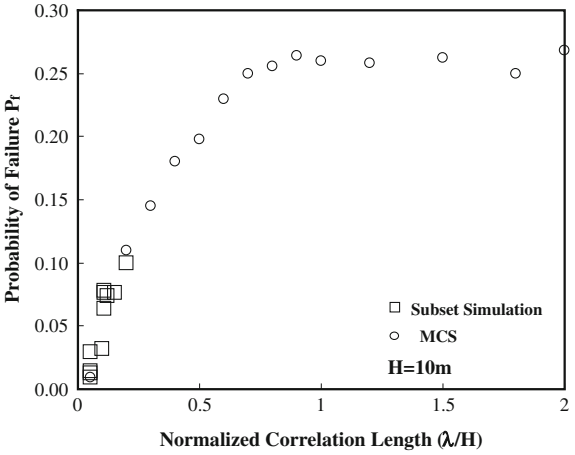

Fig. 7.9 Effect of spatial variability of soil property (after Wang et al. 2011)

$Var(M_R)$ is equal to $\sum_{i=1}^{n_R} \Delta l_i^2 \sigma_{S_{ui}}^2$. When the inherent spatial variability is ignored by assuming perfect correlation, $\rho_{ij} = 1$ and $Var(M_R)$ is equal to $\sum_{i=1}^{n_R} \Delta l_i^2 \sigma_{S_{ui}}^2 + \sum_{i,j=1}^{n_R} \sum_{i \neq j}^{n_R} \Delta l_i \Delta l_j \sigma_{S_{ui}} \sigma_{S_{uj}}$. This leads to overestimation of $Var(M_R)$ and, hence, overestimation of the FS variance.

It is important to note that overestimation of the FS variance may result in either overestimation (conservative) or underestimation (unconservative) of P_f (i.e., probability of $FS < 1$). If $FS = 1$ occurs at the lower tail of the FS probability distribution, overestimation of the FS variance leads to overestimation of P_f, and it is therefore conservative. Figure 7.9 illustrates such case, and similar results have also been reported by Sivakumar Babu and Mukesh (2004) and Hong and Roh (2008). If the location of $FS = 1$ approaches the center, or even the upper tail, of the FS probability distribution (i.e., FS is relatively low), overestimation of the FS variance leads to underestimation of P_f, and it is therefore unconservative. Griffiths and Fenton (2004) reported that when FS is relatively low and the inherent spatial variability is ignored by assuming perfect correlation, the value of P_f is underestimated and unconservative. Depending on the location of $FS = 1$ in the FS probability distribution, the overestimation of FS variance may result in contradicting results, as reported in the literature.

7.8 Effect of Critical Slip Surface Uncertainty

The discussions above show that different reliability methods deal with the critical slip surface differently. FOSM and direct MCS with Slope/W use a given slip surface and do not account for critical slip surface uncertainty. The FORM proposed by Low (2003) includes center coordinates and radius of slip surface as

additional optimization variables, and variation of potential critical slip surfaces is implicitly factored in the analysis. However, because of limitation of the optimization tool used, it tends to overestimate β and underestimate P_f.

The direct MCS and subset simulation with Excel package developed in this chapter explicitly search a wide range of potential slip surfaces for obtaining the minimum FS in each random sample of $\underline{S_u}$. Figure 7.10 shows examples of different critical slip surfaces obtained from different random samples of $\underline{S_u}$ when $\lambda = 0.5$ m. It is obvious that the critical slip surface varies spatially as the spatial distribution of $\underline{S_u}$ changes among different random samples. As a reference, the critical slip surface highlighted by a thick line in Fig. 7.10 is the one used in the FOSM method and direct MCS with Slope/W. Table 7.5 summarizes ranges of (x_c, y_c) and r for critical slip surfaces obtained from direct MCS with Excel. The r varies from 21.0 to 29.8 m and has a range of 8.8 m. When inherent spatial variability of soil property and critical slip surface uncertainty are considered explicitly in the simulation, the value of P_f from direct MCS and subset simulation with Excel is about 40–70 % larger than that from FOSM and direct MCS with Slope/W which use only one given critical slip surface.

To further illustrate the effect of critical slip surface uncertainty on P_f, direct MCS and subset simulation are also performed in Excel with the fixed critical slip surface highlighted by thick line in Fig. 7.10, which is the same one used in the direct MCS with Slope/W. As shown in Table 7.6, the resulting P_f value decreases to 0.1–0.2 % and compares well with that from Slope/W which uses the same critical slip surface. The comparison summarized in Table 7.6 confirms that when

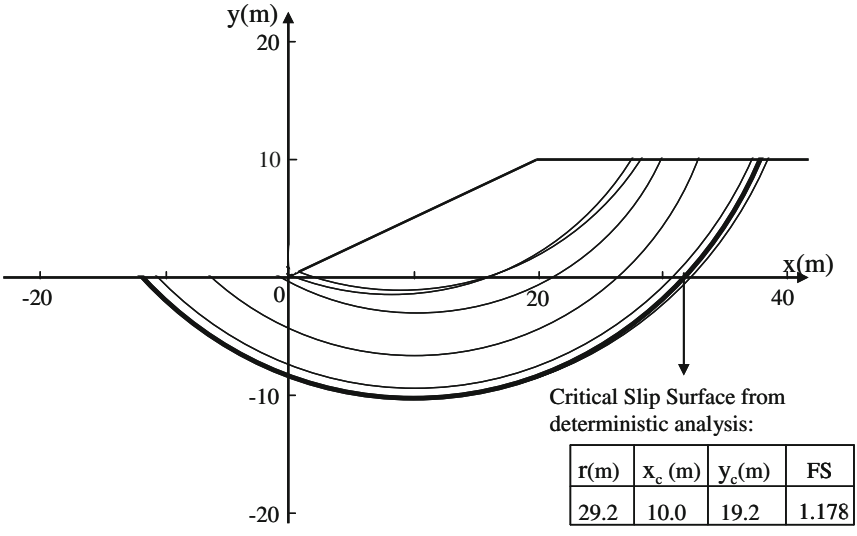

r(m)	x_c (m)	y_c(m)	FS
29.2	10.0	19.2	1.178

Fig. 7.10 Examples of critical slip surfaces obtained from direct MSC with Excel (after Wang et al. 2011)

Table 7.5 Ranges of center coordinates and radius of critical slip surfaces obtained from MCS with Excel (after Wang et al. 2011)

Parameter	Minimum	Maximum	Range
Coordinate x_c (m)	8.0	10.4	2.4
Coordinate y_c (m)	17.6	22.0	4.4
Radius r (m)	21.0	29.8	8.8

Table 7.6 Comparison of simulation results with different critical slip surfaces (after Wang et al. 2011)

Reliability method	Reliability index β	Probability of failure P_f (%)	Relative difference in P_f (%)
MCS with Slope/W and fixed critical slip surface	2.80	0.26	−73
MCS with Excel and fixed critical slip surface	2.95	0.16	−83
Subset simulation with Excel and fixed critical slip surface	3.00	0.13	−86
MCS with Excel and changing critical slip surface	2.35	0.95	N/A
Subset simulation with Excel and changing critical slip surface	2.36	0.92	−3

inherent spatial variability of soil property is considered, the substantial difference among P_f from different reliability methods is mainly attributed to the effect of critical slip surface uncertainty, and using only one given critical slip surface results in underestimation (or unconservative) of P_f. Thus, when inherent spatial variability of soil property is considered, the critical slip surface uncertainty should be properly accounted for.

7.9 Summary and Conclusions

This chapter developed a Monte Carlo simulation (MCS)-based practical reliability analysis approach for slope stability problem and implemented an advanced MCS method called subset simulation in a commonly available spreadsheet environment, Microsoft Excel. The Excel spreadsheet package developed was used to assess reliability of short-term stability of a cohesive soil slope, followed by a comparative study on different reliability methods, including the FOSM, FORM, direct MCS using commercial software Slope/W, and direct MCS and subset simulation using the Excel package. Subset simulation was shown to significantly improve efficiency and resolution of simulations at small probability levels. Such improvement

becomes increasingly substantial and necessary as the probability level of interest decreases (e.g., the failure probability further decreases to 0.1 % or 0.003 % for expected performance levels of "above average" or "good," respectively, as direct MCS is increasingly inefficient).

Effect of inherent spatial variability of soil property was explored using the Excel spreadsheet package developed in this chapter. It is found that when inherent spatial variability of soil property is ignored by assuming perfect correlation, the variance of FS is overestimated. However, the overestimation of the FS variance may result in either overestimation (conservative) or underestimation (unconservative) of P_f. If $FS = 1$ occurs at the lower tail of the FS probability distribution, overestimation of the FS variance leads to overestimation of P_f, and it is therefore conservative. If the location of $FS = 1$ approaches the center, or even the upper tail, of the FS probability distribution (i.e., FS is relatively low), overestimation of the FS variance leads to underestimation of P_f, and it is therefore unconservative.

The effect of critical slip surface uncertainty was also examined. When the inherent spatial variability of soil property is ignored or soil property is characterized by a single random variable, the location of critical slip surface is deterministic. It is therefore theoretically appropriate to use only one given slip surface in the analysis, as what FOSM method or direct MCS with Slope/W does. When the inherent spatial variability of soil property is considered, the critical slip surface varies spatially. Using only one given critical slip surface significantly underestimates P_f, and it is unconservative. Thus, when the inherent spatial variability of soil property is considered, the critical slip surface uncertainty should be properly accounted for.

It is worthwhile to note that although the proposed practical reliability analysis approach was illustrated through a cohesive soil slope example with Ordinary Method of Slices, the approach is general and can be readily adapted to frictional slopes and more sophisticated limit equilibrium methods (e.g., Spencer, Morgenstern, and Price methods). Usage of these more sophisticated methods may be more appropriate for general slopes, although their FS equations and associated discussions may not be as explicit as those (e.g., Eq. (7.4) and its relevant discussions) shown in the chapter.

References

Ang, A.H.S., and W.H. Tang. 1984. *Probability concepts in engineering planning and design*, vol. II. New York: Wiley.

Au, S.K., and J.L. Beck. 2001. Estimation of small failure probabilities in high dimensions by subset simulation. *Probabilistic Engineering Mechanics* 16(4): 263–277.

Au, S.K., and J.L. Beck. 2003. Subset simulation and its applications to seismic risk based on dynamic analysis. *Journal of Engineering Mechanics* 129(8): 1–17.

Au, S.K., Z. Cao, and Y. Wang. 2010. Implementing advanced Monte Carlo simulation under spreadsheet environment. *Structural Safety* 32(5): 281–292.

Au, S.K., J. Ching, and J.L. Beck. 2007. Application of subset simulation methods to reliability benchmark problems. *Structural Safety* 29(3): 183–193.

Au, S.K., Y. Wang, and Z. Cao. 2009. Reliability analysis of slope stability by advanced simulation with spreadsheet. In *Proceedings of the Second International Symposium on Geotechnical Safety and Risk*. Gifu, Japan, June 2009, 275–280.

Ching, J.Y., K.K. Phoon, and Y.H. Hsieh. 2009. Reliability analysis of a benchmark problem for 1-D consolidation. In *Proceeding of the 2nd International Symposium on Geo-technical Safety and Risk (IS-Gifu2009)*, June 2009, Gifu, Japan, 69–74.

Duncan, J.M. and S.G. Wright. 2005. *Soil strength and slope stability*. New Jersey: Wiley.

El-Ramly, H., N.R. Morgenstern, and D.M. Cruden. 2002. Probabilistic slope stability analysis for practice. *Canadian Geotechnical Journal* 39: 665–683.

El-Ramly, H., N.R. Morgenstern, and D.M. Cruden. 2005. Probabilistic assessment of stability of a cut slope in residual soil. *Geotechnique* 55(1): 77–84.

GEO-SLOPE International Ltd. 2008. *Stability modeling with slope/W 2007 version*. Calgary, Alberta, Canada: GEO-SLOPE International Ltd.

Griffiths, D.V., and G.A. Fenton. 2004. Probabilistic slope stability analysis by finite elements. *Journal of Geotechnical and Geoenvironmental Engineering* 130(5): 507–518.

Hassan, A.M., and T.F. Wolff. 1999. Search algorithm for minimum reliability index of earth slopes. *Journal of Geotechnical and Geoenvironmental Engineering* 125(4): 301–308.

Hong, H.P., and G. Roh. 2008. Reliability evaluation of earth slopes. *Journal of Geotechnical and Geoenvironmental Engineering* 134(12): 1700–1705.

Low, B.K. 2003. Practical probabilistic slope stability analysis. In *Proceeding of 12th Panamerican Conference on Soil Mechanics and Geotechnical Engineering and 39th U.S. Rock Mechanics Symposium*, 2777–2784. Cambridge, Massachusetts: MIT Press, Verlag Gluckauf Gmbh Essen.

Low, B.K., and W.H. Tang. 2007. Efficient spreadsheet algorithm for first-order reliability method. *Journal of Engineering Mechanics* 133(2): 1378–1387.

Metropolis, N., A. Rosenbluth, M. Rosenbluth, and A. Teller. 1953. Equations of state calculations by fast computing machines. *Journal of Chemical Physics* 21(6): 1087–1092.

Robert, C. and G. Casella. 2004. *Monte Carlo Statistical Methods*. Springer.

Sivakumar Babu, G.L., and M.D. Mukesh. 2004. Effect of soil variability on reliability of soil slopes. *Geotechnique* 54(5): 335–337.

Tang, W.H., M.S. Yucemen, and A.H.S. Ang. 1976. Probability based short-term design of slope. *Canadian Geotechnical Journal* 13: 201–215.

Vanmarcke, E.H. 1977. Probabilistic modeling of soil profiles. *Journal of Geotechnical Engineering* 103(11): 1127–1246.

Vanmarcke, E.H. 1983. *Random fields: analysis and synthesis*. Cambridge: MIT Press.

Wang, Y., and Z. Cao. 2013. Probabilistic characterization of Young's modulus of soil using equivalent samples. *Engineering Geology* 159(12): 106–118.

Wang, Y., Z. Cao, and S.K. Au. 2011. Practical analysis of slope stability by advanced Monte Carlo Simulation in spreadsheet. *Canadian Geotechnical Journal* 48(1): 162–172.

Wu, T.H. 2008. Reliability analysis of slopes. In *Reliability-based design in geotechnical engineering: computations and applications*, Chapter 11, ed. Phoon, 413–447. Taylor and Francis.

Xu, B., and B.K. Low. 2006. Probabilistic stability analyses of embankments based on finite-element method. *Journal of Geotechnical and Geoenvironmental Engineering* 132(11): 1444–1454.